



Mitochondrial dysfunction in kidney stones and relief of kidney stones after reducing mtROS

Yuexian Xu^{1,2,3} · Guoxiang Li^{1,2,3} · Defeng Ge^{1,2,3} · Yan Chen⁴ · Bingbing Hou^{1,2,3} · Zongyao Hao^{1,2,3}

Received: 27 June 2024 / Accepted: 6 August 2024

© The Author(s), under exclusive licence to Springer-Verlag GmbH Germany, part of Springer Nature 2024

Abstract

Mitochondria are essential organelles because they generate the energy required for cellular functions. Kidney stones, as one of the most common urological diseases, have garnered significant attention. In this study, we first collected peripheral venous blood from patients with kidney stones and used qRT-PCR to detect mitochondrial DNA (mtDNA) copy number as a means of assessing mitochondrial function in these patients. Subsequently, through Western blotting, qPCR, immunofluorescence, immunohistochemistry, and transmission electron microscopy, we examined whether calcium oxalate crystals could cause mitochondrial dysfunction in the kidney in both in vitro and in vivo. We then examined the intersection of the DEGs obtained by transcriptome sequencing of the mouse kidney stone model with mitochondria-related genes, and performed KEGG and GO analyses on the intersecting genes. Finally, we administered the mitochondrial ROS scavenger Mito-Tempo in vivo and observed its effects. Our findings revealed that patients with kidney stones had a reduced mtDNA copy number in their peripheral venous blood compared to the control group, suggesting mitochondrial dysfunction in this population. This conclusion was further validated through in vitro and in vivo experiments. Enrichment analyses revealed that the intersecting genes were closely related to metabolism. We observed that after mitochondrial function was preserved, the deposition of calcium oxalate crystals decreased, and the kidney damage and inflammation caused by them were also alleviated. Our research indicates that kidney stones can cause mitochondrial dysfunction. After clearing mtROS, the damage and inflammation caused by kidney stones are reversed, providing new insights into the prevention and treatment of kidney stones.

Keywords Kidney stones · Mitochondrial dysfunction · Mitochondrial copy number

Yuexian Xu, Guoxiang Li and Defeng Ge contributed equally to this work.

✉ Yan Chen
276117277@qq.com

✉ Bingbing Hou
binggoaza@163.com

✉ Zongyao Hao
haozongyao@ahmu.edu.cn

¹ Department of Urology, The First Affiliated Hospital of Anhui Medical University, Hefei, China

² Institute of Urology, Anhui Medical University, Hefei, China

³ Anhui Province Key Laboratory of Urological and Andrological Diseases Research and Medical Transformation, Anhui Medical University, Hefei, China

⁴ Department of General Practice, Wuhu City Second People's Hospital, Wuhu, China

Introduction

Kidney stones are prevalent in nearly every part of the world, and their occurrence is increasing in certain regions [1–4]. There is a greater prevalence of kidney stones in males than in females [5]. Currently, kidney stones can be treated effectively through various methods. Among them, surgical options like extracorporeal shock wave lithotripsy (ESWL), transurethral ureteroscopic lithotripsy (TUL), and percutaneous nephrolithotomy (PCNL) are widely used. The selection of the appropriate treatment mainly relies on the stone's size and position [6]. However, recurrence after stone removal remains a significant challenge in the surgical management of kidney stones. The recurrence rate of kidney stones is as high as 50% [7]. The cost of stone removal is quite high, and in addition to the economic burden, kidney stones also place a significant physical and mental strain

on patients [8]. Therefore, understanding the pathogenesis of kidney stones is a very important research approach.

Mitochondria are widely recognized as crucial for eukaryotic life, earning the nickname “powerhouses of the cell” due to their role in generating a majority of the cell’s energy or ATP. These organelles possess their own genome, known as mtDNA, which replicates independently from the host’s genetic material [9]. In contrast to nuclear DNA, mitochondrial DNA (mtDNA) is circular and double-stranded, lacking the protection of histones, thus increasing its vulnerability to damage [10, 11]. It is widely acknowledged that mitochondrial damage and dysfunction play pivotal roles in contributing to a multitude of chronic and acute renal diseases [12]. Mitochondrial dysfunction is linked to inflammation, fibrosis, and kidney damage [13–15]. However, research exploring the connection between mitochondrial dysfunction and kidney stone disease remains relatively scarce.

This study aids in clarifying the significance of mitochondrial function in kidney stone pathology and contributes to the advancement of novel kidney stone treatment approaches, ultimately improving patients’ quality of life and easing the public health burden.

Materials and methods

Chemicals and reagents

Beta actin (20536-1-AP), PGC1a (66369-1-Ig), TFAM (22586-1-AP), TOMM20 (11802-1-AP) and CYTB (55090-1-AP) were obtained from Proteintech (Wuhan, China). DRP1 (#DF7037) and p-DRP1 (#DF2980) were obtained from Affinity Biosciences. Anti-4 Hydroxynonenal (ab46545) was obtained from Abcam (America). Mito-Tempo (MT, a mtROS scavenger) was purchased from TargetMol (Shanghai, China) and was dissolved in DMSO as a stock solution.

Collection of clinical samples

After the Ethics Committee of the First Affiliated Hospital of Anhui Medical University approval (Number: Quick-PJ2024-05-91), we randomly selected 20 adult patients who were first diagnosed with kidney stones and 20 healthy controls. The exclusion criteria were diabetes, hypertension, hyperlipidemia, preoperative fever, preoperative urinary tract infection, and renal insufficiency, coagulation dysfunction, abnormal liver function, anemia. 5 ml venous blood of the subjects was drawn on an empty stomach in the morning and stored at -80 °C for future examination.

Cell culture and treatment

The human kidney cell line (HK-2) was provided by the Institute of Basic Medical Sciences of the Chinese Academy of Medical Sciences. These cells were routinely cultured in DMEM/F12 mixed medium in an environment containing 5% CO₂ and 95% humidity. For the purpose of experimentation, we stimulated the HK-2 cells with COM at a concentration of 100 µg/ml for 24 h [16].

DNA isolation and mtDNA copy number assay

The mtDNA copy number was determined by qPCR following a previously established described [17]. In summary, we extracted total DNA from blood samples using a universal genomic DNA kit (Model: CW2298S, Manufacturer: CWBIO, Beijing, China). Subsequently, we took 10ng of DNA samples for qPCR analysis. To determine the copy number of mtDNA, we amplified the mitochondrial ND1 gene (mtND1) and normalized it to the nuclear β -2 microglobulin (B2M) gene for comparison. The primers used in this study are detailed in Supplementary Table 1.

Animals and experimental design

This study employed male C57BL/6J mice aged between 6 and 8 weeks as experimental subjects, sourced from the highly reputable Experimental Animal Center of Anhui Medical University. To ensure consistency and reliability, all related animal experiments were conducted under strict supervision at the center. Prior to commencing the experiment, explicit approval was obtained from the Animal Experimentation Ethics Committee of Anhui Medical University, with an approval number of LLSC20232250. Throughout the entire study, internationally recognized guidelines for the use and care of laboratory animals were consistently followed, safeguarding animal welfare and ethical experimentation. To establish a mouse model of CaOx deposition, precise intraperitoneal injections of Glyoxylic acid (Gly) at a dose of 100 mg/kg will be administered to each mouse. This process will continue for 7 days, conducted at regular intervals daily to ensure model consistency and stability. Intraperitoneal injection of MT (5 mg/kg, dissolved in PBS containing 5% DMSO) is administered daily six hours before Gly injection. After completing the 7-day injection cycle, the mice will be euthanized for subsequent analysis and research. This process strictly adheres to relevant regulations and ethical guidelines, ensuring experimental safety and humanity. In summary, through professional animal sourcing and management, rigorous experimental design, precise execution of key steps, and strict adherence to experimental ethics and regulations, this

study aimed to achieve scientific research objectives while prioritizing animal welfare [18]. Kidneys were harvested for subsequent experiments. The renal tissue was embedded in paraffin according to standard procedures and was then used for molecular analysis.

Western blot analysis

Initially, we separated 25 micrograms of tissue lysate using 10% SDS-PAGE and then transferred it to an NC membrane via electrophoretic transfer. Following this, we blocked the membrane for 2 h using a Tris-buffered saline solution containing 0.05% Tween 20 and 5% skim milk. After the blocking step, the NC membrane was incubated with a specific primary antibody for 8 h. Subsequently, at 37 °C, the membrane was incubated with a secondary antibody for 120 min. Finally, we imaged the results using the Licor/Odyssey infrared imaging system (model ChemiScope 5600, provided by Hengmei Technology, China) and quantified the gray values of each band using ImageJ software.

Immunohistochemistry

After standard histopathological processing, we prepared paraffin-embedded mouse kidney sections. This procedure included fixation with 4% paraformaldehyde, dehydration, wax infiltration, paraffin embedding, and finally sectioning to a thickness of 4 micrometers. To ensure experimental accuracy, we effectively inhibited the endogenous peroxidase activity of the kidney sections before incubation. Subsequently, the sections were incubated with anti-4-HNE antibodies overnight at 4 °C to ensure sufficient reaction. After that, the sections were co-incubated with the secondary antibody for 50 min at room temperature, further enhancing the antigen-antibody reaction. Finally, we visualized the results using DAB staining. All microscopic images were captured with high precision using the Olympus IX83 microscope from Japan to ensure image quality.

RNA extraction and real-time PCR

Total RNA was extracted from renal tissue and cells by utilizing Trizol (Gibco, Life Technologies, CA, USA) and subsequently reverse transcribed into cDNA through the application of the iScript cDNA Synthesis Kit (Bio-Rad, USA). Real-time quantitative PCR was conducted by employing Bio-Rad iQ SYBR Green Supermix and Opticon two, within the CFX96 real-time RT-PCR detection system (Bio-Rad, USA). For reference, the primers utilized in this investigation are enumerated in Supplementary Table 1.

Immunofluorescence staining

Cell and tissue sections were mounted on slides, immobilized with paraformaldehyde, and then exposed to anti-TFAM and anti-TOM20 antibodies overnight at 4 °C. After rinsing with PBS, the cells were dyed with 4',6-diamidino-2-phenylindole (DAPI). Following a 2-hour incubation, they were treated with the corresponding secondary antibody at 37 °C. Images were captured using a fluorescence microscope (Olympus IX83, Japan).

Transmission electron microscope

Samples of cells and tissues, which were stabilized with 2.5% glutaraldehyde, were dehydrated, embedded, cured, and subsequently sliced into ultrathin sections measuring 50–60 nm. The resulting specimens were examined using a transmission Electron Microscope (Hitachi, Tokyo, Japan) for imaging.

Detection of renal CaOx crystals

Deposits of CaOx crystals were observed on the renal surfaces stained with HE, visualized in polarized light optical micrographs (Zeiss, Oberkochen, Germany).

Mitotracker staining

Following treatment, HK-2 cells underwent labeling with Mitotracker Red CMXRos (obtained from Beyotime Biotechnology, Shanghai, China) to pinpoint mitochondria. These cells were exposed to a Mitotracker working solution at a 100 nM concentration for a duration of 20 min at 37 °C. Subsequently, the cells were stabilized using 4% paraformaldehyde for 15 min. Prior to analyzing the images under a fluorescence microscope, the cells were rinsed three times with PBS.

Data source

A total of 1136 mitochondrial related genes (Mito-RGs) were obtained from the Molecular Signatures Database (MSigDB) (<http://software.broadinstitute.org/gsea/msigdb>) [19]. The RNA-seq data analyzed in this study originated from four mice each in the control and model groups that we established. OE Biotech Co., Ltd (Shanghai, China) conducted the sequencing.

Table 1 General information of subjects

	Control	Kidney stone patient	<i>p</i>
Age(year)	35.90 ± 10.18	43.05 ± 14.01	0.0726
Sex			> 0.9999
Males	10	10	
Females	10	10	
BMI (kg/m ²)	22.49 ± 1.676	22.35 ± 1.842	0.8029
Blood glucose(mmol/L)	4.985 ± 0.7464	4.990 ± 0.7312	0.983
CRE(μmol/L)	64.70 ± 9.905	63.85 ± 10.78	0.7965
ALT(U/L)	27.60 ± 8.947	26.75 ± 7.765	0.7501
AST(U/L)	25.20 ± 6.014	24.90 ± 5.428	0.8693

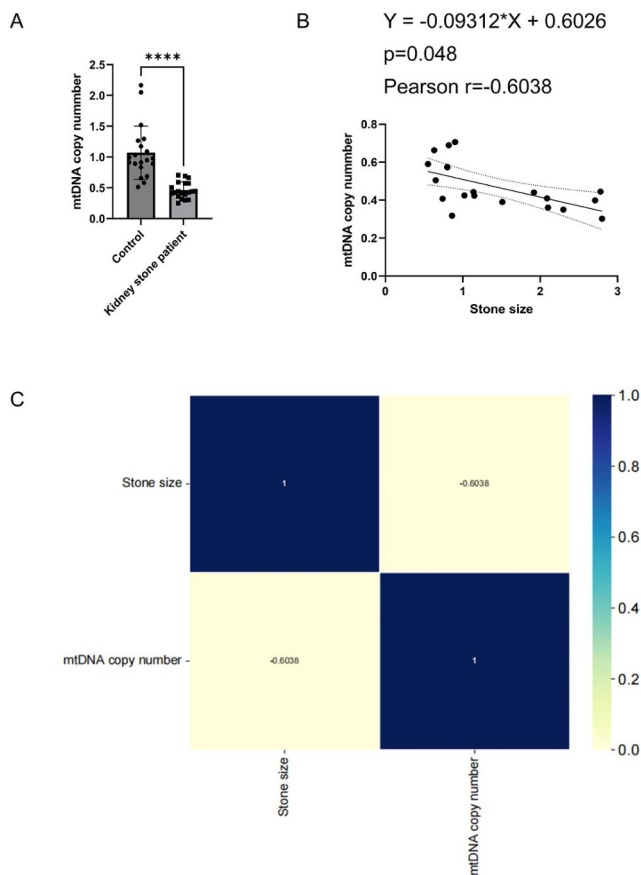


Fig. 1 The mtDNA copy number in the blood of patients with kidney stones is lower than that of the control group. **A:** Comparison of mitochondrial DNA copy number between stone patients and control group. **B:** The linear correlation equation between stone size and mtDNA copy number, with the dashed line representing the range of the 95% confidence interval. **C:** Heatmap of the Pearson correlation coefficient between Stone size and mtDNA copy number. **p* < 0.05, ***p* < 0.01, ****p* < 0.001, *****p* < 0.0001 compared with the medium control

Construction of intersecting gene interaction networks and screening of key genes

The STRING database (<https://cn.string-db.org/>) serves as a platform for assessing protein-protein interactions (PPI) among potential targets. PPI network visualization becomes possible by importing STRING data into Cytoscape 3.7 software. In addition, the Cytohubba plug-in is used to identify key genes.

Enrichment analysis

Enrichment analysis was performed on 142 targets using the David data platform (<https://david.ncifcrf.gov/home.jsp>), and online biological tools were utilized to visually represent the results.

Statistical analysis

The differences among the groups were evaluated using one-way analysis of variance (ANOVA), conducted with GraphPad Prism 8.3.0 software (GraphPad Software, San Diego, CA, USA).

Results

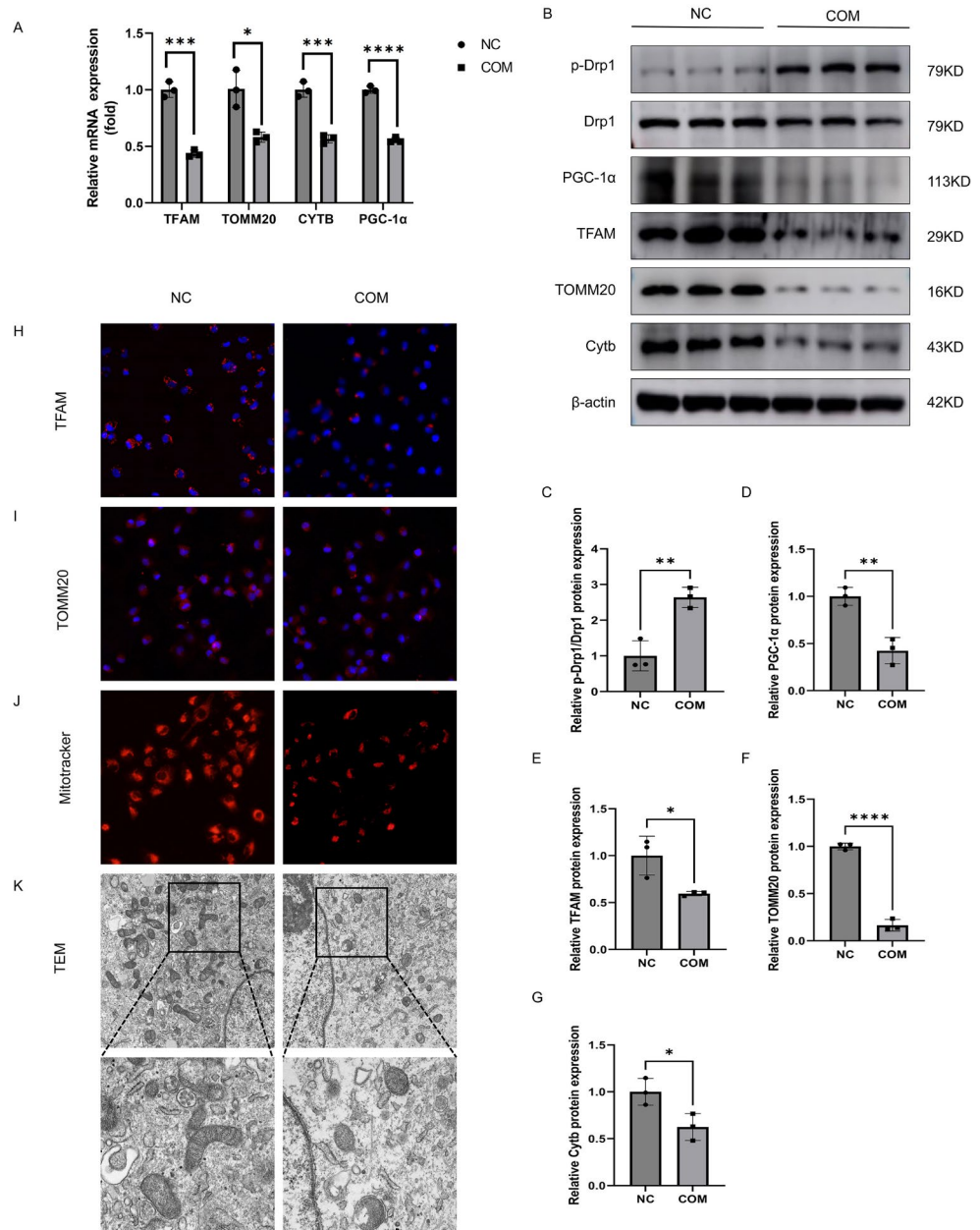
The mtDNA copy number in the blood of patients with kidney stones is lower than that of the control group

The general information of the subjects included in this study can be found in Table 1. Through the collection of peripheral venous blood from patients with kidney stones for mtDNA copy number detection, we found that the mtDNA copy number in the peripheral venous blood of patients with kidney stones was significantly reduced compared to the control group (Fig. 1A). Then we discovered that there might be a negative correlation between stone size and mtRNA, and there exists a linear relationship between them (Fig. 1B). The P-value of the linear equation is 0.048. Furthermore, we conducted a Pearson correlation analysis and obtained a correlation coefficient of $r = -0.6038$ (Fig. 1C).

COM induces mitochondrial dysfunction in HK2 cells

We stimulated HK2 cells with COM crystals and RT-PCR analysis revealed that COM crystals induced changes in the mRNA expression levels of TFAM, TOMM20, Cytb, and PGC-1 α (Fig. 2A). We then discovered through Western blotting that COM causes a reduction in the protein expression levels of TFAM, TOMM20, Cytb, and PGC-1 α , while

Fig. 2 COM induces mitochondrial dysfunction in HK2 cells. **(A)** Changes in mRNA expression levels of PGC-1 α , TOMM20, TFAM, and Cytb in the control group and model group of HK2 cells. **(B–G)** Changes in protein expression levels of p-Drp1/Drp, PGC-1 α , TFAM, TOMM20, and Cytb in the control group and model group of HK2 cells. **(H, I)** Immunofluorescence of TFAM and TOMM20 in the control group and model group of HK2 cells. **(J)** MitoTracker staining of HK2 cells in the control group and model group. **(K)** Observation of mitochondrial morphology in control group and model group cells by transmission electron microscopy. The data are shown as the mean \pm S.E.M. of at least 3 biological replicates. * $p < 0.05$, ** $p < 0.01$, *** $p < 0.001$, **** $p < 0.0001$ compared with the medium control



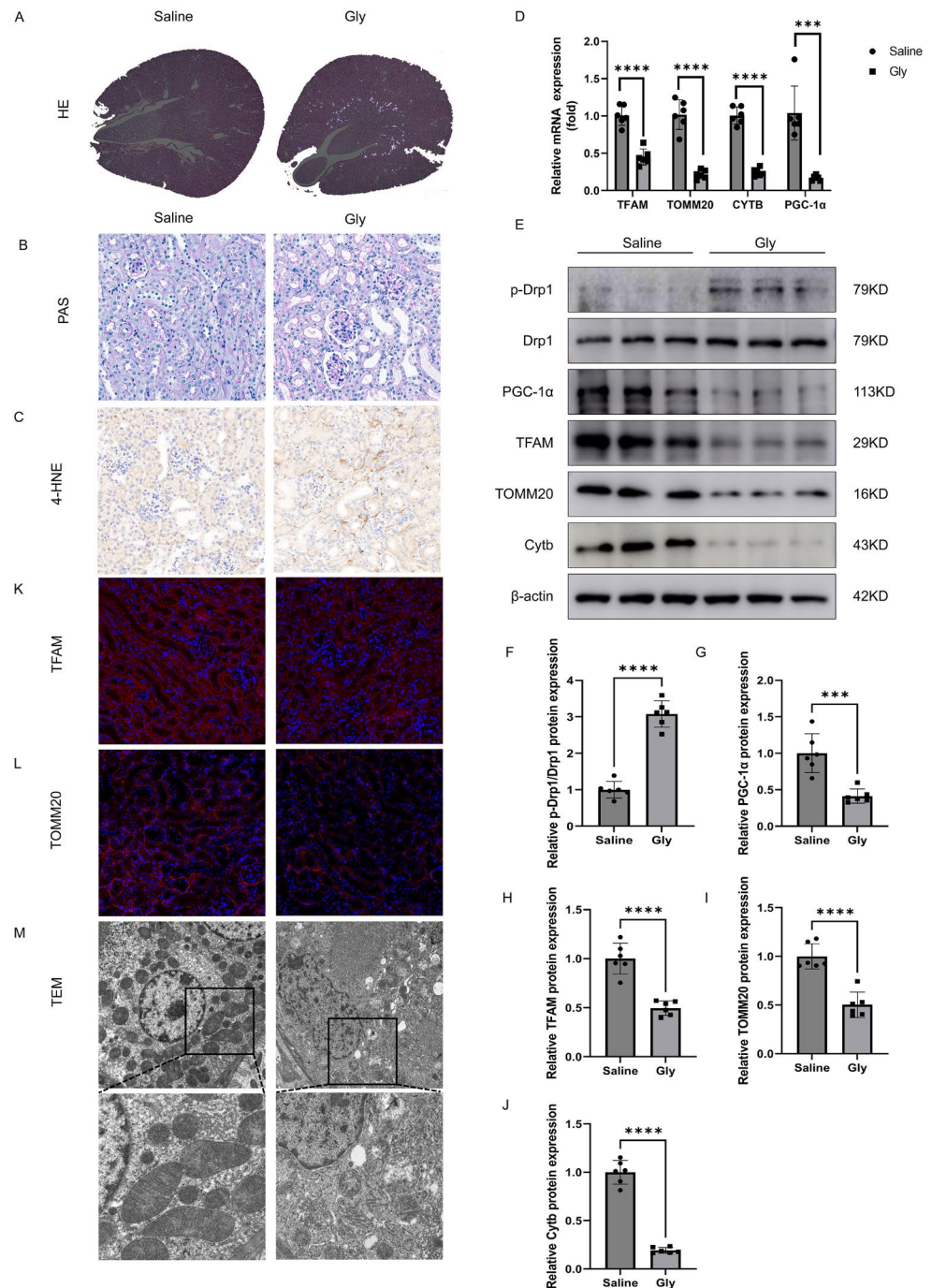
increasing the phosphorylation level of DRP1 (Fig. 2B–G). This indicates that HK2 cells exhibit mitochondrial dysfunction following stimulation with COM. The immunofluorescence results of TFAM and TOMM20 further confirmed this conclusion (Fig. 2H, I). We used MitoTracker Deep Red staining to analyze the mitochondria of the cells and employed electron microscopy to examine the ultrastructure of the mitochondria. As shown in Fig. 2J, the mitochondrial mass of HK2 cells stimulated by COM significantly decreased. As shown in Fig. 2K, COM reduced the number of healthy mitochondria and induced abnormalities in mitochondrial morphology, such as mitochondrial swelling,

fragmentation, membrane integrity disruption, and crista absence.

Calcium oxalate crystal deposition causes impaired mitochondrial function in mouse kidneys

We constructed an animal model of calcium oxalate crystal deposition by intraperitoneal injection of glyoxylate, a model widely used to study the effects of calcium oxalate stones on the kidneys [20–22]. After HE staining and observation under polarized light microscopy, we found extensive CaOx crystal deposition in the model group (Fig. 3A). PAS staining revealed severe pathological damage to the

Fig. 3 Calcium oxalate crystal deposition causes impaired mitochondrial function in mouse kidneys. **(A)** Observe the deposition of CaOx crystals in the kidneys of the model group using polarized light microscopy. **(B)** Assess renal tubule damage in the kidneys of mice in the model group using PAS staining. **(C)** Immunohistochemical images showing changes in 4-HNE expression levels in the kidneys of mice in the model group. **(D)** Changes in mRNA expression levels of PGC-1 α , TOMM20, TFAM, and Cytb in renal tissues of the model group and control group. **(E–J)** Changes in protein expression levels of p-Drp1/Drp, PGC-1 α , TFAM, TOMM20, and Cytb in the kidneys of the model group and control group. **(K, L)** Immunofluorescence detection of TFAM and TOMM20 proteins in renal tissues of the model group and control group. **(M)** Observe the morphological changes of mitochondria in kidney cells of the model group and control group using transmission electron microscopy. The data are shown as the mean \pm S.E.M. of at least 3 biological replicates. * $p < 0.05$, ** $p < 0.01$, *** $p < 0.001$, **** $p < 0.0001$ compared with the medium control



renal tubular epithelial cells of mice after exposure to CaOx, with the kidneys of the model group showing disorganized tubular structures, lumen expansion, loss of brush borders, vacuolization changes in cells, and separation from the lumen (Fig. 3B). 4-HNE staining confirmed the production of ROS in the model kidneys (Fig. 3C). We then measured changes in mRNA and protein levels of mitochondrial function-related indicators in kidney tissues. Through RT-PCR, we found that the mRNA expression levels of TFAM,

TOMM20, Cytb, and PGC-1 α were significantly decreased in the model group (Fig. 3D). WB results showed a reduction in the protein levels of TFAM, TOMM20, Cytb, and PGC-1 α , while the phosphorylation level of DRP1 increased (Fig. 3E–J). The immunofluorescence results of TFAM and TOMM20 in kidney tissues also yielded consistent findings (Fig. 3K, L). This aligns with the results from the aforementioned in vitro experiments, indicating that CaOx can induce mitochondrial dysfunction in the kidney. We then observed

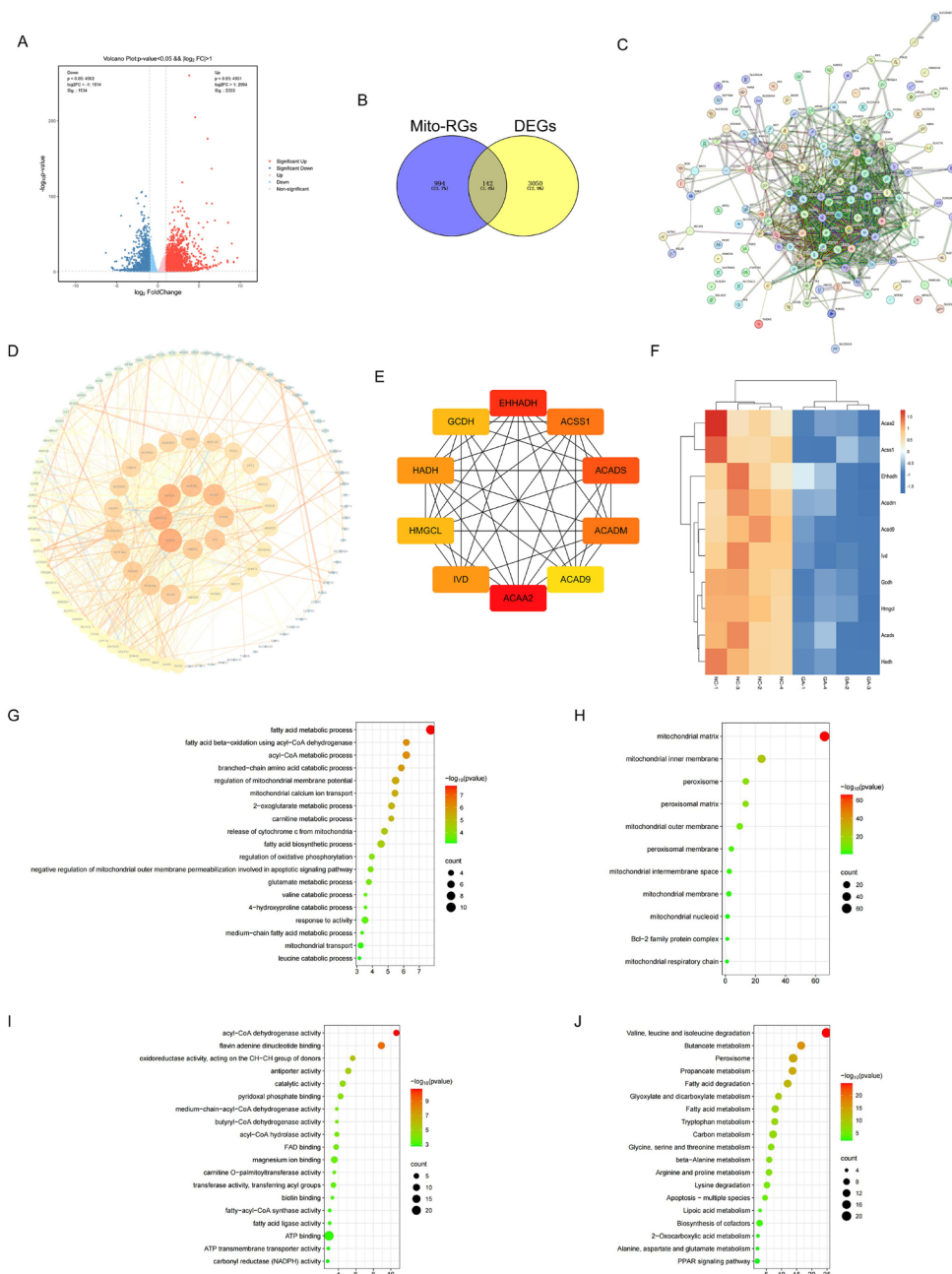
changes in the mitochondria within renal tubular epithelial cells using transmission electron microscopy and noted a significant reduction in the number of mitochondria and clear morphological changes in the model group (Fig. 3M).

Network and enrichment analysis of the intersection between differentially expressed genes in kidney stones and mitochondrial-related genes

We obtained 3192 differentially expressed genes between the two groups through gene expression RNAseq, with selection criteria of P-value < 0.01 and |log₂ FC| > 1 (Fig. 4A).

Among these differentially expressed genes, 142 genes overlap with mitochondrial-related genes (Fig. 4B). Using the STRING online platform, we constructed an interaction network among the 142 intersecting genes (Fig. 4C). Subsequently, we obtained the network graph and data from the platform, and then imported this information into Cytoscape 3.7 for further analysis (Fig. 4D). The screening of key genes was completed through the application of the Cytohubba plugin (Fig. 4E). The heatmap display of HUB genes is shown in Fig. 4F. The GO pathway enrichment analysis of the 142 mitochondria-related DEGs revealed that, in terms of biological process (BP), the DEGs were primarily

Fig. 4 Network and enrichment analysis of the intersection between differentially expressed genes in kidney stones and mitochondrial-related genes. **(A)** Volcano plot of kidney RNA-seq sequencing in model mice and control group. **(B)** Venny diagram showing the intersection of differentially expressed genes and mitochondrial-related genes. **(C, D)** Protein-protein interaction network of intersecting genes. **(E)** Presentation of hub genes. **(F)** Heatmap display of HUB genes. **(G–I)** GO analysis of intersecting genes. **(J)** KEGG analysis of intersecting genes



enriched in fatty acid metabolic processes, fatty acid beta-oxidation utilizing acyl-CoA dehydrogenase, and acyl-CoA metabolic processes (Fig. 4G). When considering cellular component (CC), the DEGs showed significant enrichment in the mitochondrial matrix, mitochondrial inner membrane, and peroxisome pathways (Fig. 4H). For molecular function (MF), the DEGs were linked to acyl-CoA dehydrogenase activity, as well as oxidoreductase activity affecting the CH-CH group of donors (Fig. 4I). KEGG enrichment analysis revealed a significant number of metabolism-related pathways among these identified pathways (Fig. 4J).

After reducing mtROS, mitochondrial dysfunction and kidney damage caused by kidney stones are alleviated

To investigate the role of mtROS in mitochondrial damage caused by kidney stones, we used the mtROS scavenger MT *in vivo*. We found that the deposition of calcium oxalate crystals decreased significantly (Fig. 5A), PAS staining showed significant relief of kidney damage (Fig. 5B), and inflammation in the kidney was also reversed (Fig. 5C). Immunofluorescence revealed that MT alleviated the decrease in TFAM and TOMM20 in the kidney (Fig. 5D, E). Then, through WB, we found that MT significantly alleviated the decreases in TFAM, TOMM20, PGC-1 α , Cytb, and the increase in the p-DRP1/DRP1 ratio (Fig. 5F–K).

Discussion

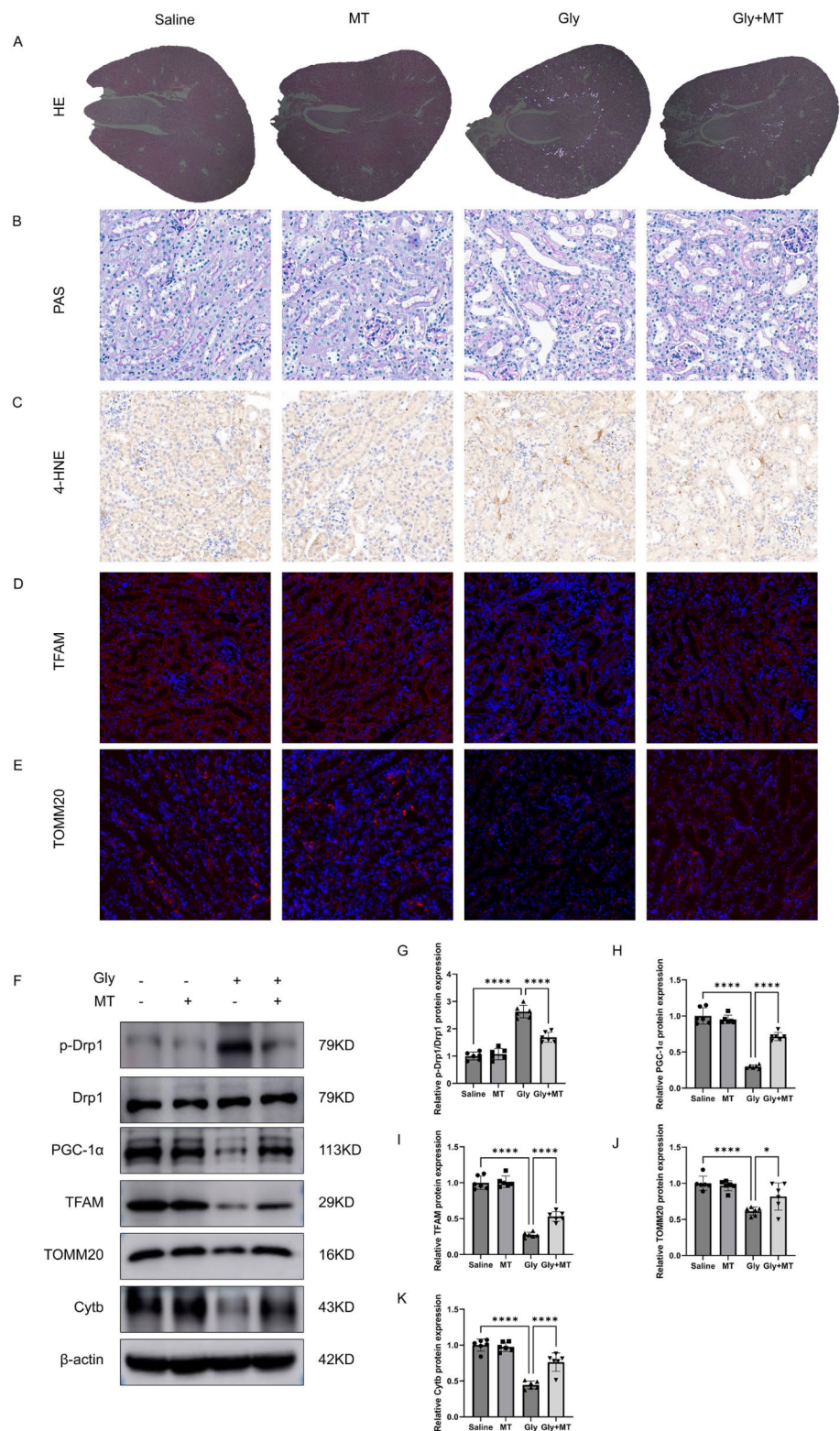
In this study, first, we discovered that the mtDNA copy number in the peripheral venous blood of patients with kidney stones is reduced, and then confirmed through *in vitro* and *in vivo* experiments that kidney stones indeed impair mitochondrial function. Finally, we took the intersection of the differentially expressed genes from the model and mitochondrial-related genes to obtain overlapping genes, and analyzed them.

The kidneys eliminate metabolic waste by utilizing the glomerular filtration barrier and preserve water-electrolyte equilibrium through tubular reabsorption mechanisms [23]. Kidneys, as high-energy demanding organs, possess a large mitochondrial population for ATP production, maintaining their internal homeostasis [24]. An expanding collection of research indicates that mitochondrial malfunction has a significant impact on the initiation and advancement of kidney disorders, specifically acute kidney injury (AKI) and chronic kidney disease (CKD) [14, 17, 25]. However, the alterations in mitochondrial function within the context of kidney stone disease have not been well elucidated.

Mitochondria play a pivotal role in human cells, functioning as tiny power plants within the cell responsible for energy production [26]. Mitochondria play a crucial role in cellular activities. They effectively regulate intracellular oxidative stress, helping cells cope with various oxidative pressures. Meanwhile, mitochondria also maintain intracellular calcium homeostasis, ensuring stability within the cellular environment. In addition, mitochondria are involved in the apoptotic signaling pathway, regulating the normal cell death process. It's worth mentioning that mitochondria also play a key role in the aging process of all cells and tissues, exerting a profound influence on the overall health and lifespan of organisms [27, 28].

Previous studies have focused mainly on kidney stones that induce oxidative stress in the kidneys, leading to renal tubular epithelial cell damage [18, 29–31]. Oxidative stress occurs when there is an imbalance between the increased production of reactive oxygen species (ROS) and the decreased ability of the antioxidant defense system to neutralize them [32]. The accumulation of reactive oxygen species (ROS) in the organism, coupled with an imbalance in redox reactions, can adversely affect a variety of crucial biomolecules, including proteins, nucleic acids, carbohydrates, and lipids. This situation may trigger functional disorders in these biomolecules and even lead to their oxidation. Such oxidation and dysregulation have the potential to impair cellular functions, ultimately having a negative impact on the organism's health. In summary, excessive accumulation of ROS and redox imbalance are significant contributors to biomolecular dysregulation and oxidation, which may result in cellular damage and health issues [33]. The imbalance of intracellular and extracellular environments triggered by oxidative stress may induce apoptosis or necrosis of cells, which may further cause tissue damage. It is worth noting that oxidative stress has been proven by multiple studies to be a core factor in the pathophysiology of acute and chronic kidney diseases. Its critical role is not only reflected in the pathogenesis of kidney diseases, but also throughout the progression and prognosis of the diseases. Therefore, a deep exploration of the role of oxidative stress in kidney diseases is of great significance for understanding the essence of the disease and developing new treatment strategies. Relevant literature and research have extensively explored the close connection between oxidative stress and kidney health, further supporting the key role of oxidative stress in kidney diseases [34, 35]. Endogenous reactive oxygen species are primarily produced in the mitochondria of our body cells [36]. Increasing evidence suggests that mitochondria are the primary source of intracellular ROS, with approximately 90% of ROS being generated in mitochondria [27]. Mitochondria are like “small power plants” within the cell, and the electron transport chain is a crucial component of these

Fig. 5 After reducing mtROS, mitochondrial dysfunction and kidney damage caused by kidney stones are alleviated. **(A)** Observe the changes in CaOx crystal deposition in the kidneys after mtROS removal using polarized light microscopy. **(B)** Evaluate the changes in the degree of renal tubular injury after mtROS clearance using PAS staining. **(C)** Immunohistochemical images showing changes in 4-HNE protein in renal tissues after mtROS clearance. **(D, E)** Immunohistochemical images showing changes in TFAM and TOMM20 proteins in the kidneys of the model group after mtROS clearance. **(F–K)** Changes in protein expression levels of p-Drp1/Drp, PGC-1 α , TFAM, TOMM20, and Cytb in renal tissues after mtROS clearance. The data are shown as the mean \pm S.E.M. of at least 3 biological replicates. * $p < 0.05$, ** $p < 0.01$, *** $p < 0.001$, **** $p < 0.0001$ compared with the medium control



“power plants,” playing a very important role in the production of ROS. Of course, ROS have other sources. For instance, NADPH oxidase on the cell membrane, xanthine oxidoreductase in peroxisomes within the cell, and protein

disulfide isomerase involved in the processing of misfolded proteins in the endoplasmic reticulum can all generate ROS. In addition, there are some enzymatic reactions, such as prostaglandin synthesis, self-oxidation of epinephrine, and

the reduction process of riboflavin, which can also contribute to the production of ROS [37].

Significantly distinct from nuclear DNA, human mitochondrial DNA (mtDNA) exhibits a unique circular structure and precisely consists of 16,569 base pairs. This genetic material is meticulously divided into two complementary strands, referred to as the heavy strand and the light strand. These strands carry crucial information for encoding the essential protein subunits of the mitochondrial oxidative phosphorylation system (OXPHOS). However, it's worth noting that due to the lack of histone protection and defense mechanisms in the coding region, mtDNA becomes particularly sensitive to oxidative stress, significantly increasing its susceptibility [38]. In our study, we observed a significant decrease in mitochondrial DNA (mtDNA) levels in the serum of kidney stone patients compared to the healthy control group. It's worth noting that this finding has also been validated in related studies on other kidney diseases. Numerous research data indicate that diabetic patients also show a similar downward trend in serum mtDNA. These discoveries suggest that serum mtDNA levels may be closely related to the pathophysiology of kidney diseases and diabetes [15, 39, 40]. Liu Y and his colleagues, through a large-scale cohort study of elderly people, found that a decrease in mtDNA copy number is a potential risk factor for CKD [41]. Liu J found that mtDNA copy number is associated with better kidney function and less pathological damage in patients with IgA nephropathy [42].

A large number of studies have demonstrated the important role of mitochondrial dysfunction in many other kidney diseases through *in vivo* and *in vitro* experiments [17, 43–45]. Then, through *in vitro* experiments, we discovered that after stimulating HK2 cells with COM, we stained the cells with MitoTracker, a mitochondrial fluorescent dye. Compared to the control group, the mitochondria became more fragmented after COM stimulation. The expression levels of mitochondrial function-related proteins also changed. The results from transmission electron microscopy further indicated that mitochondrial function was impaired in HK2 cells after COM stimulation. Next, we conducted *in vivo* experiments for verification. Calcium oxalate accounts for the highest proportion of kidney stones, so we constructed a calcium oxalate crystal deposition model *in vivo*. Through testing, we found that calcium oxalate crystals induced mitochondrial dysfunction in the kidney.

Then, we obtained differentially expressed genes by performing transcriptome sequencing analysis on the kidneys of mice in both the model group and the control group. Following this, we intersected these genes with mitochondrial-related genes and conducted enrichment analysis on the intersecting genes. We found that the intersecting genes are closely related to a large number of metabolism-related

pathways. It has long been known that mitochondrial metabolism is crucial for bioenergetics, and its metabolism is multifaceted, reflecting a variety of functions. The kidney is an organ with intense metabolic activity, harboring a higher concentration of mitochondria per unit weight than any other organ, excluding the heart. We believe that kidney stones may cause mitochondrial dysfunction through metabolic changes [28]. We provide a specific direction for studying mitochondrial dysfunction in kidney stones, laying a foundation for subsequent research. Finally, we found that mtROS scavengers can alleviate mitochondrial dysfunction, thereby mitigating the formation and damage of kidney stones.

Treatment strategies for patients with kidney stones may need to consider the importance of protecting mitochondrial function. Antioxidant therapy, improving microcirculation, and targeted metabolic interventions could help alleviate mitochondrial dysfunction and may serve as adjunctive measures to prevent the formation of kidney stones or reduce their size. In this study, the number of clinical samples included is limited. The animal model we use cannot fully simulate the formation of kidney stones in humans. However, due to current limitations in experimental methods, most researchers consider this model to be the closest animal model to the real situation. In future research, we will continue to explore models that can better simulate the formation of kidney stones to further our studies. In subsequent studies, we need to expand the sample size and continue to investigate the specific mechanism of mitochondrial dysfunction caused by kidney stones, as well as its potential as a pharmacological target.

Conclusion

In summary, kidney stones can cause mitochondrial dysfunction, and mitochondrial-related targets may provide new insights for the prevention and treatment of kidney stones.

Supplementary Information The online version contains supplementary material available at <https://doi.org/10.1007/s00240-024-01614-y>.

Acknowledgements This study was supported by the National Natural Science Foundation of China (grant number 82074394 and 82370768) and the Science and Technology Project Foundation of Wuhu (2023jc33).

Author contributions Yuexian Xu and Guoxiang Li: Writing-original draft. Defeng Ge and Yan Chen: Data collection and analysis. Bingbing Hou: Revise the original draft. Zongyao Hao: Supervision. All the authors agreed for the final version to be published.

Data availability No datasets were generated or analysed during the current study.

Declarations

Ethics statement The animal study was reviewed and approved by The Animal Experimentation Ethics Committee of Anhui Medical University (No: LLSC20232250).

Informed consent Informed consent was obtained from all subjects involved in the study.

Competing interests The authors declare no competing interests.

References

- Gadzhiev N, Prosyannikov M, Malkhasyan V, Akopyan G, Somani B, Sivkov A, Apolikhin O, Kaprin A (2021) Urolithiasis prevalence in the Russian Federation: analysis of trends over a 15-year period. *World J Urol* 39:3939–3944. <https://doi.org/10.1007/s00345-021-03729-y>
- Karagiannis A, Skolarikos A, Alexandrescu E et al (2017) Epidemiologic study of urolithiasis in seven countries of South-Eastern Europe: S.E.G.U.R. 1 study. *Arch Ital Urol Androl* 89:173–177. <https://doi.org/10.4081/aiua.2017.3.173>
- Wang Q, Wang Y, Yang C, Wang J, Shi Y, Wang H, Zhang L, Zhao MH (2023) Trends of Urolithiasis in China: a national study based on hospitalized patients from 2013 to 2018. *Kidney Dis (Basel)* 9:49–57. <https://doi.org/10.1159/000527967>
- Lang J, Narendrula A, El-Zawahry A, Sindhwanji P, Ekwenna O (2022) Global trends in incidence and burden of urolithiasis from 1990 to 2019: an analysis of global burden of disease study data. *Eur Urol Open Sci* 35:37–46. <https://doi.org/10.1016/j.euros.2021.10.008>
- Abufaraj M, Xu T, Cao C et al (2021) Prevalence and Trends in kidney stone among adults in the USA: analyses of national health and nutrition examination survey 2007–2018 data. *Eur Urol Focus* 7:1468–1475. <https://doi.org/10.1016/j.euf.2020.08.011>
- Peerapen P, Thongboonkerd V (2023) Kidney stone prevention. *Adv Nutr* 14:555–569. <https://doi.org/10.1016/j.advnut.2023.03.002>
- Kachkoul R, Touimi GB, El Mouhri G, El Habbani R, Mohim M, Lahrichi A (2023) Urolithiasis: history, epidemiology, aetiologic factors and management. *Malays J Pathol* 45:333–352
- Stern KL, Gao T, Antonelli JA et al (2019) Association of patient age and gender with kidney stone related quality of life. *J Urol* 202:309–313. <https://doi.org/10.1097/JU.0000000000000291>
- Annesley SJ, Fisher PR (2019) Mitochondria in health and disease. *Cells* 8:680. <https://doi.org/10.3390/cells8070680>
- Sharma P, Sampath H (2019) Mitochondrial DNA integrity: role in health and disease. *Cells* 8:100. <https://doi.org/10.3390/cells8020100>
- Yan C, Duanmu X, Zeng L, Liu B, Song Z (2019) Mitochondrial DNA: distribution, mutations, and elimination. *Cells* 8:379. <https://doi.org/10.3390/cells8040379>
- Ratliff BB, Abdulmahdi W, Pawar R, Wolin MS (2016) Oxidant mechanisms in renal injury and disease. *Antioxid Redox Signal* 25:119–146. <https://doi.org/10.1089/ars.2016.6665>
- Chung KW, Dhillon P, Huang S et al (2019) Mitochondrial damage and activation of the STING pathway lead to renal inflammation and fibrosis. *Cell Metab* 30:784–799e5. <https://doi.org/10.1016/j.cmet.2019.08.003>
- Maekawa H, Inoue T, Ouchi H et al (2019) Mitochondrial damage causes inflammation via cGAS-STING signaling in acute kidney injury. *Cell Rep* 29:1261–1273e6. <https://doi.org/10.1016/j.celrep.2019.09.050>
- Xiao L, Xu X, Zhang F et al (2017) The mitochondria-targeted antioxidant MitoQ ameliorated tubular injury mediated by mitophagy in diabetic kidney disease via Nrf2/PINK1. *Redox Biol* 11:297–311. <https://doi.org/10.1016/j.redox.2016.12.022>
- Liu H, Ye T, Yang X et al (2019) H19 promote calcium oxalate nephrocalcinosis-induced renal tubular epithelial cell injury via a ceRNA pathway. *EBioMedicine* 50:366–378. <https://doi.org/10.1016/j.ebiom.2019.10.059>
- Zhao M, Wang Y, Li L et al (2021) Mitochondrial ROS promote mitochondrial dysfunction and inflammation in ischemic acute kidney injury by disrupting TFAM-mediated mtDNA maintenance. *Theranostics* 11:1845–1863. <https://doi.org/10.7150/thno.50905>
- Yan Q, Hu Q, Li G, Qi Q, Song Z, Shu J, Liang H, Liu H, Hao Z (2023) NEAT1 regulates calcium oxalate crystal-induced renal tubular oxidative injury via miR-130/IRF1. *Antioxid Redox Signal* 38:731–746. <https://doi.org/10.1089/ars.2022.0008>
- Zhang T, Nie Y, Gu J, Cai K, Chen X, Li H, Wang J (2021) Corrigendum: identification of mitochondrial-related prognostic biomarkers associated with primary bile acid biosynthesis and tumor microenvironment of hepatocellular carcinoma. *Front Oncol* 11:843623. <https://doi.org/10.3389/fonc.2021.843623>
- Duan X, Kong Z, Mai X et al (2018) Autophagy inhibition attenuates hyperoxaluria-induced renal tubular oxidative injury and calcium oxalate crystal depositions in the rat kidney. *Redox Biol* 16:414–425. <https://doi.org/10.1016/j.redox.2018.03.019>
- Liu H, Duan C, Yang X, Liu J, Deng Y, Tiselius HG, Ye Z, Wang T, Xing J, Xu H (2023) Metformin suppresses calcium oxalate crystal-induced kidney injury by promoting Sirt1 and M2 macrophage-mediated anti-inflammatory activation. *Signal Transduct Target Ther* 8:38. <https://doi.org/10.1038/s41392-022-01232-3>
- Liu H, Yang X, Tang K et al (2020) Sulforaphane elicits dual therapeutic effects on renal inflammatory injury and crystal deposition in calcium oxalate nephrocalcinosis. *Theranostics* 10:7319–7334. <https://doi.org/10.7150/thno.44054>
- Wang K, Kestenbaum B (2018) Proximal tubular secretory clearance: a neglected partner of kidney function. *Clin J Am Soc Nephrol* 13:1291–1296. <https://doi.org/10.2215/CJN.12001017>
- Mao J, Li C, Wu F, Wang Y, Zhu J, Wen C (2024) The relationship between kidney disease and mitochondria: a bibliometric study. *Ren Fail* 46:2302963. <https://doi.org/10.1080/0886022X.2024.2302963>
- Srivastava A, Tomar B, Sharma D, Rath SK (2023) Mitochondrial dysfunction and oxidative stress: role in chronic kidney disease. *Life Sci* 319:121432. <https://doi.org/10.1016/j.lfs.2023.121432>
- Alevriadou BR, Patel A, Noble M, Ghosh S, Gohil VM, Stathopoulos PB, Madesh M (2021) Molecular nature and physiological role of the mitochondrial calcium uniporter channel. *Am J Physiol Cell Physiol* 320:C465–C482. <https://doi.org/10.1152/ajpcell.00502.2020>
- Bhargava P, Schnellmann RG (2017) Mitochondrial energetics in the kidney. *Nat Rev Nephrol* 13:629–646. <https://doi.org/10.1038/nrneph.2017.107>
- Duann P, Lin PH (2017) Mitochondria damage and kidney disease. *Adv Exp Med Biol* 982:529–551. https://doi.org/10.1007/978-3-319-55330-6_27
- Kang J, Sun Y, Deng Y, Liu Q, Li D, Liu Y, Guan X, Tao Z, Wang X (2020) Autophagy-endoplasmic reticulum stress inhibition mechanism of superoxide dismutase in the formation of calcium oxalate kidney stones. *Biomed Pharmacother* 121:109649. <https://doi.org/10.1016/j.biopha.2019.109649>

30. Liu J, Huang J, Gong B et al (2023) Polydatin protects against calcium oxalate crystal-induced renal injury through the cytoplasmic/mitochondrial reactive oxygen species-NLRP3 inflammasome pathway. *Biomed Pharmacother* 167:115621. <https://doi.org/10.1016/j.biopha.2023.115621>
31. Gao M, Meng T, Chen F et al (2024) Inhibitory effect of *Incarvillea Diffusa* Royle extract in the formation of calcium oxalate nephrolithiasis by regulating ROS-induced Nrf2/HO-1 pathway in rats. *J Ethnopharmacol* 325:117619. <https://doi.org/10.1016/j.jep.2023.117619>
32. Zorov DB, Juhaszova M, Sollott SJ (2014) Mitochondrial reactive oxygen species (ROS) and ROS-induced ROS release. *Physiol Rev* 94:909–950. <https://doi.org/10.1152/physrev.00026.2013>
33. Bonventre JV, Weinberg JM (2003) Recent advances in the pathophysiology of ischemic acute renal failure. *J Am Soc Nephrol* 14:2199–2210. <https://doi.org/10.1097/01.asn.0000079785.13922.f6>
34. Fan Y, Yuan Y, Xiong M et al (2023) Tet1 deficiency exacerbates oxidative stress in acute kidney injury by regulating superoxide dismutase. *Theranostics* 13:5348–5364. <https://doi.org/10.7150/thno.87416>
35. Li S, Gu X, Zhang M, Jiang Q, Xu T (2024) Di (2-ethylhexyl) phthalate and polystyrene microplastics co-exposure caused oxidative stress to activate NF-κB/NLRP3 pathway aggravated pyroptosis and inflammation in mouse kidney. *Sci Total Environ* 926:171817. <https://doi.org/10.1016/j.scitotenv.2024.171817>
36. Sureshbabu A, Ryter SW, Choi ME (2015) Oxidative stress and autophagy: crucial modulators of kidney injury. *Redox Biol* 4:208–214. <https://doi.org/10.1016/j.redox.2015.01.001>
37. Donate-Correa J, Martín-Carro B, Cannata-Andía JB, Mora-Fernández C, Navarro-González JF (2023) Klotho, oxidative stress, and mitochondrial damage in kidney disease. *Antioxid (Basel)* 12:239. <https://doi.org/10.3390/antiox12020239>
38. West AP, Shadel GS (2017) Mitochondrial DNA in innate immune responses and inflammatory pathology. *Nat Rev Immunol* 17:363–375. <https://doi.org/10.1038/nri.2017.21>
39. Jenkins AJ, Carroll LM, Huang M, Wen-Loh Y, Mangani A, O'Neal DN, Januszewski AS (2023) Mitochondrial DNA copy number in adults with and without type 1 diabetes. *Diabetes Res Clin Pract* 203:110877. <https://doi.org/10.1016/j.diabres.2023.110877>
40. Petrica L, Vlad A, Gadalean F et al (2023) Mitochondrial DNA changes in blood and urine display a specific signature in relation to inflammation in normoalbuminuric diabetic kidney disease in type 2 diabetes Mellitus patients. *Int J Mol Sci* 24:9803. <https://doi.org/10.3390/ijms24129803>
41. Liu Y, Pan Y, Tian Z, Wang J, Chen F, Geng Z, Li Q, Liu Z, Zhou X, Zhou K (2023) Association of mitochondrial DNA copy number with chronic kidney disease in older adults. *BMC Geriatr* 23:514. <https://doi.org/10.1186/s12877-023-04203-7>
42. Liu J, Wang R, Luo N, Li Z, Mao H, Zhou Y (2023) Mitochondrial DNA copy number in peripheral blood of IgA nephropathy: a cross-sectional study. *Ren Fail* 45:2182133. <https://doi.org/10.1080/0886022X.2023.2182133>
43. Miao J, Huang J, Luo C, Ye H, Ling X, Wu Q, Shen W, Zhou L (2021) Klotho retards renal fibrosis through targeting mitochondrial dysfunction and cellular senescence in renal tubular cells. *Physiol Rep* 9:e14696. <https://doi.org/10.14814/phy2.14696>
44. Oh CJ, Kim MJ, Lee JM et al (2023) Inhibition of pyruvate dehydrogenase kinase 4 ameliorates kidney ischemia-reperfusion injury by reducing succinate accumulation during ischemia and preserving mitochondrial function during reperfusion. *Kidney Int* 104:724–739. <https://doi.org/10.1016/j.kint.2023.06.022>
45. Yu B, Jin L, Yao X et al (2023) TRPM2 protects against cisplatin-induced acute kidney injury and mitochondrial dysfunction via modulating autophagy. *Theranostics* 13:4356–4375. <https://doi.org/10.7150/thno.84655>

Publisher's Note Springer Nature remains neutral with regard to jurisdictional claims in published maps and institutional affiliations.

Springer Nature or its licensor (e.g. a society or other partner) holds exclusive rights to this article under a publishing agreement with the author(s) or other rightsholder(s); author self-archiving of the accepted manuscript version of this article is solely governed by the terms of such publishing agreement and applicable law.